Science Press

ARTICLE

Effect of Heat Treatment on Microstructures and Tensile Properties of a New High Strength Titanium Alloy

Sheng Jinwen[1],   Wang Zhenyu[1],   Wu Di[1],   Bai Weimin[1],   Zhang Ligang[1,2],
Liu Libin [1,3]

[1] Central South University, Changsha 410083, China; [2] ZIK Virtuhcon, Technische Universität Bergakademie Freiberg, Fuchsmühlenweg 9, D-09596 Freiberg, Germany; [3] Key Laboratory of Non-ferrous Metallic Materials Science and Engineering, Ministry of Education, Changsha 410083, China

Abstract: The microstructure and mechanical properties of a high strength titanium alloy (Ti-6Al-6Mo-4V) were investigated. The relationship between microstructures and properties of the alloys was investigated after solution treatment at α/β and β regions and then aging at five different temperatures ranging from 460 to 620 °C for 6 h. The results illustrate the alloys after α/β region solution treatment and aging show a more attractive combination of strength and elongation than after β solution treatment and aging. After solution treatment at 850 °C (α/β region) and aging at 460 °C, the alloy obtains the highest strength (1572 MPa) with elongation (2.63%). When aging at 620 °C, the alloy obtains the highest elongation (11.46%) but lower strength (1201 MPa). After solution treatment at 825 °C plus aging at 540 °C, this alloy reaches a great combination of strength (1328 MPa) and elongation (7.58%). Meanwhile, because the large β grains form after β region solution treatment and fine secondary α forms during aging, it does not obtain an attractive strength after β region solution treatment plus aging.

Key words: Ti-6Al-6Mo-4V; microstructures; mechanical properties; fracture surface

Owing to their lightweight, high corrosion resistance, high specific strength and toughness, titanium and titanium alloys have become one of the most attractive structural materials[1-3]. In the recent years, many types of titanium alloys have been widely developed, especially for the aerospace industry. The high strength and high fracture toughness are still the first requirements, but the poor matching of comprehensive mechanical properties is an urgent problem for many new alloys. For example, because of the limitation of low elongation, many types of titanium alloys cannot be used at a high strength level. Such as, the Ti-13V-11Cr-3A1, which is a type of commercial beta titanium alloy developed for a fighter, but it is then being replaced due to the poor elongation (2%) at 1240 MPa strength level[4]. On the contrary, Ti-6Al-4V is another kind of commercial $\alpha+\beta$ titanium alloy which has been widely used because of good comprehensive mechanical properties, especially for its good elongation, but its moderate

strength (< 1000 MPa) determines that it cannot meet any requirements for high strength[5]. So, to develop a new type of titanium alloy with great combination of high strength and good elongation is an urgent job. As mentioned above, Ti-6Al-4V has good comprehensive mechanical properties except for low strength[6-8]. This problem can be overcomed by addition of alloying elements to Ti-6Al-4V alloy.

In order to achieve a high strength level, Molybdenum (Mo) as a kind of β stabilizer element is widely used for alloying because of its function of precipitation strengthening effect, which will promote the formation of metastable β phase after rapid cooling and result in the precipitation of acicular α phase during aging treatment[9]. The work of Andrew Boyne et al.[10] described the Pseudospinodal mechanism of fine alpha/beta microstructure in Ti-Mo alloys, which resulted in a very fine structure. What is more, researchers also proved that Mo element could enhance the mechanical properties of the titanium alloys[11,12]. For example,

Ti-Mo alloys have excellent mechanical properties which were reported by Oliveira et al.[13] and Rodrigues et al.[14] And molybdenum is also an environmentally friendly element[5]. Therefore, molybdenum could be a suitable element to modify the Ti-6Al-4V alloy. Actually, the molybdenum has been successfully applied to many alloys as an alloying element, such as Ti-5553 (Ti-5Mo-5A1-5V-3Cr)[15,16] and Ti-7333 (Ti-7Mo-3Al-3Cr-3Nb)[17].

In this work, the objective of molybdenum addition is to increase the strength while maintaining the original good comprehensive mechanical properties of Ti6Al4V alloy. Hence, Ti-664 (Ti-6Al-6Mo-4V) as a new titanium alloy was designed to satisfy the requirements. Generally, the microstructures are sensitive to heat treatment process. In order to reach a good combination of high strength and elongation, it is necessary to control the microstructure of titanium alloy throughout heat treatment process. So, this paper focuses on the fundamental research on the microstructure and properties of the new alloy (Ti-664) by heat treatment process and aims to establish the relationship of microstructures and properties.

1   Materials and Methods

The Ti-6Al-6Mo-4V alloy was melted by double vacuum arc re-melting (VAR). The ingot was firstly forged at 1000 °C (β region) to a square rod. Then, the blocks were forged for the third time at around 830 °C (α/β region) with about 80% deformation for tensile samples. Fig.1 shows the microstructure and XRD pattern of the alloy after being forged. The alloy consists of continuous β phase and spherically α_p phase (primary α) after forging at α/β region. Table 1 is the chemical composition of the alloy that was measured by the wet analysis method. And, it is a type of $\alpha+\beta$ titanium alloy according to the value of Molybdenum equivalent which is about 8.86[18]. The β transus temperature of the alloy was found to be (875±5) °C by metallographic method.

A vacuum tube furnace was used for samples heat treatment process. The JEOL-JSM 7001F Field Emission Gun-Scanning Electron Microscope (FEG-SEM) and FEI Titan 80-300 microscope (TEM) were used to reveal microstructures under suitable working conditions. Tensile specimens were made according to the standard size requirements after heat treatment. MTS810 was selected as a testing machine in room temperature tensile tests with speed of 2 mm/min.

2   Results and Discussion

2.1   Microstructures

The microstructures in Fig.2 show the alloy after solution treatment at 825, 850 and 900 °C followed by air cooling. The α/β region heat treatment retains the two-phase microstructures (Fig.2a and 2b) compared to the β region heat treatment (Fig.2c). Furthermore, after solution treatment at 825 °C/0.5 h/AQ, the volume fraction of primary α is around 29.6%, and it decreases to around
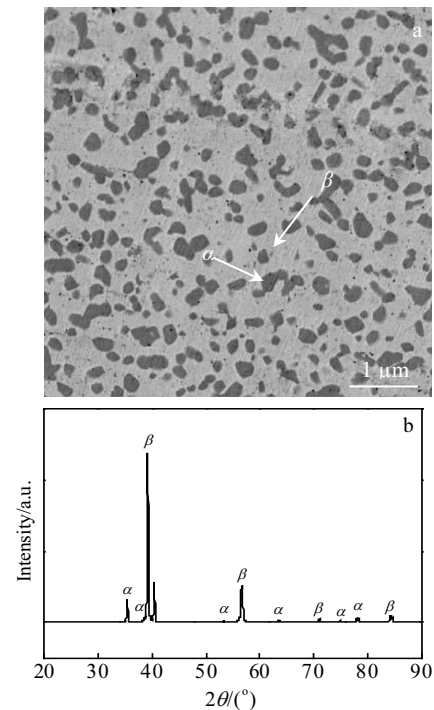
Fig.1   SEM image (a) and XRD pattern (b) of as-received alloy along the transversal section

Table 1   Chemical composition of the Ti664 alloy (wt%)

Al	Mo	V	C	O	Ti
5.63	5.91	4.45	0.023	0.183	Bal.
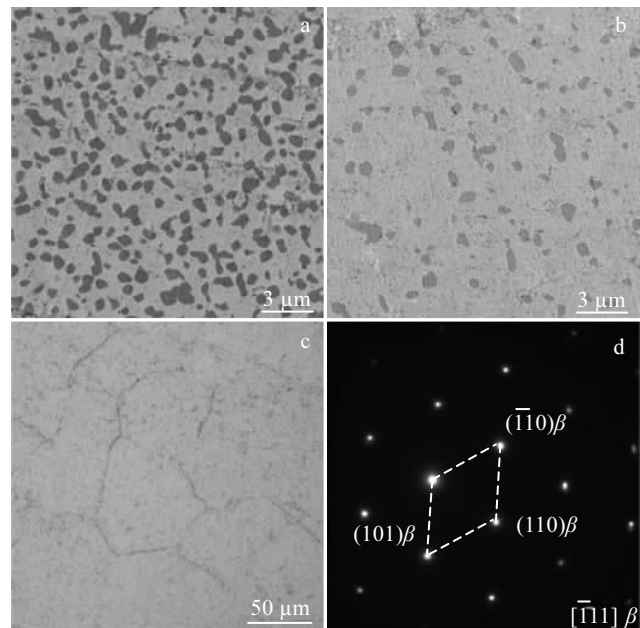
Fig.2   Microstructures (a~c) and SAED pattern (d) of solution treated alloy along the transversal section with different treatment regimes: (a) 825 °C/0.5 h; (b) 850 °C/0.5 h; (c) 900 °C/0.5 h

14.3% after solution treatment at 850 $^{\circ}$C/0.5 h/AQ. The average lobular α size after solution treatment at 820 $^{\circ}$C was measured to be about 0.94 μm, and it is 1.25 μm after solution treatment at 850 $^{\circ}$C. It is because the higher solution treatment temperature provided larger diffusion force for the spheroidization of primary α which leads to larger average size of primary α[19]. It has been reported that the α_p phase plays an important role in limiting the growth of β grains by pinning the original β grain boundaries and reducing their mobility[20]. And it is clear to see that the α_p phase homogeneously distributed in the β matrix (Fig.2a and 2b). So, the β phase is limited effectively, which can be known from the size of β grains.

On the contrary, large and equiaxed β grains with size of around 100 μm to 150 μm were obtained after β region solution treatment (Fig.2c). And the $[\overline{1}11]$ β zone axis selected area diffraction pattern in Fig.2d shows that the α phase totally dissolves. This type of microstructure had been found in many works after β region solution treatment[4,8,20].

Fig.3 and Fig.4 show the microstructures of the alloy after α/β solution treatment (825 and 850 $^{\circ}$C) plus aging at different temperatures for 6 h. The variation tendency for microstructure is same for two different solution conditions. During the process of aging, the acicular shape secondary α phase formed in the matrix, as indicated by arrows in Fig.3 and Fig.4. After aging at 460 and 500 $^{\circ}$C, the secondary α phases are too fine to be observed in SEM images (Fig.3a and 3b, Fig.4a and Fig.4b). The size of α precipitates during the process of aging are decided by the solution treatment in

α/β region. The precipitation of primary α phase is beneficial to the stability improvement of β matrix and the formation driving force reduction of the secondary α[8]. Furthermore, low aging temperatures do not provide enough driving force for the growth of the secondary α. When aging at 540 $^{\circ}$C, the fine secondary α is visible from SEM images under this condition. After aging at higher temperatures (580 and 620 $^{\circ}$C), the secondary α coarsening is visible clearly. The width of secondary α in different heat treatment conditions can be seen clearly from SEM images in Fig.3 and Fig.4, which present a tendency that the width of secondary α increases with the increase of aging temperatures for both solution treatment conditions. Furthermore, when aging at higher aging temperatures, both within the grains and along the grain boundaries precipitate the secondary α. Meanwhile, the β grain size of solution treatment at 825 $^{\circ}$C is smaller (2~4 μm) in comparison to solution treatment at 850 $^{\circ}$C (5~8 μm) (Fig.3 and Fig.4). Because more primary α at lower solution treatment temperature can restrict the β grain size effectively, which result in smaller β grains.

It is also clear to see that the secondary α precipitation after solution treatment at 850 $^{\circ}$C is much more and finer compared to after solution treatment at 825 $^{\circ}$C under the same aging conditions. The reason is that the β stabilizing elements are enriched in the β phase due to elemental partitioning. As shown in Fig.5, the composition distribution curves of quantitative statistics by EPMA suggest that the elemental
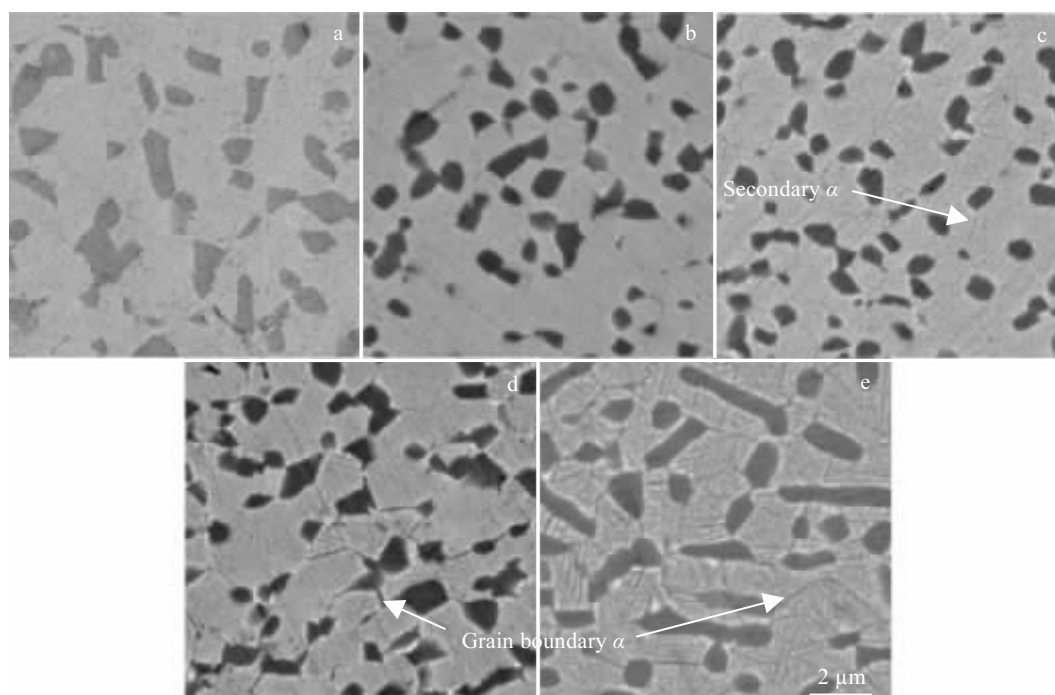
Fig.3　SEM images of the alloy after solution treatment at 825 $^{\circ}$C and aging for 6 h at different temperatures: (a) 460 $^{\circ}$C, (b) 500 $^{\circ}$C, (c) 540 $^{\circ}$C, (d) 580 $^{\circ}$C, and (e) 620 $^{\circ}$C

partitioning between α and β phases take place during quenching. Solute redistribution takes place within the β phase and forms solute rich and lean regions. Where the Al atoms are mainly enriched in α phase, while the Mo and V atoms are enriched in β phase. Therefore, the β phase is rendered more stably and the precipitation kinetics of secondary α phase formation during aging becomes sluggish under lower solution treatment condition. On the contrary, solution treatment at higher temperature becomes more unstable when comparing to the lower solution treatment condition, which will provide more energy for nucleation, resulting in finer secondary α[21]. Researchers also confirm that Mo element can refine the structure by thermodynamic calculation and simulation because of the Pseudospinodal effect[10].

Fig.6 shows that the α_s plates have two different orientations: an angle of 60° when aging at 540 °C and an angle of 90° at 580 and 620 °C. It proves that the size and volume fraction of secondary α are strongly determined by the aging temperature. The selected area electron diffraction (SAED) pattern of the $[\bar{1}11]$ zone axis of β phase after 0.5 h of aging at 540 °C is shown in Fig.6b. The presence of SAED spots from α can be distinctly visualized at the 1/2rd position along {110} diffracted spot in Fig.6b. And the selected area electron diffraction patterns of [023] β and [001] β zone axis in Fig.6d and 6f are corresponded to the microstructures in Fig.6c and 6e, respectively.

2.2 Tensile properties

Fig.7a and 7b show the tensile properties of the alloy after solution treatment at 825 and 850 °C plus aging conditions respectively. The strength and elongation vary with aging temperatures (Fig.7a) after solution treatment at 825 °C plus aging at different temperatures. The highest strength is obtained after aging at 460 °C, the ultimate tensile strength is 1431 MPa with a poor elongation (5.1%). When aging at 620 °C, the ultimate tensile strength is 1201 MPa but a good elongation is gained (11.5%). For solution treatment at 850 °C plus aging at different temperatures (Fig.7b), the highest strength is also obtained after aging at 460 °C (1572 MPa), which is higher than solution treatment at 825 °C for the same aging condition.

As mentioned above, the size of secondary α precipitation after solution treatment at 850 °C is finer than after solution treatment at 825 °C, which leads to higher strength and lower elongation (2.6%). The other reason is that larger β grains after solution treatment at 850 °C lead to a larger place for the precipitation of secondary α and then increase the volume of grain boundary of secondary α and β. Plastic deformation depends on the movement of dislocation, which is easily blocked at grain boundaries, resulting in the dislocation strengthening effect. When aging at 620 °C after solution treatment at 850 °C, the alloy gains a medium elongation (7.0%) and strength (1206 MPa).
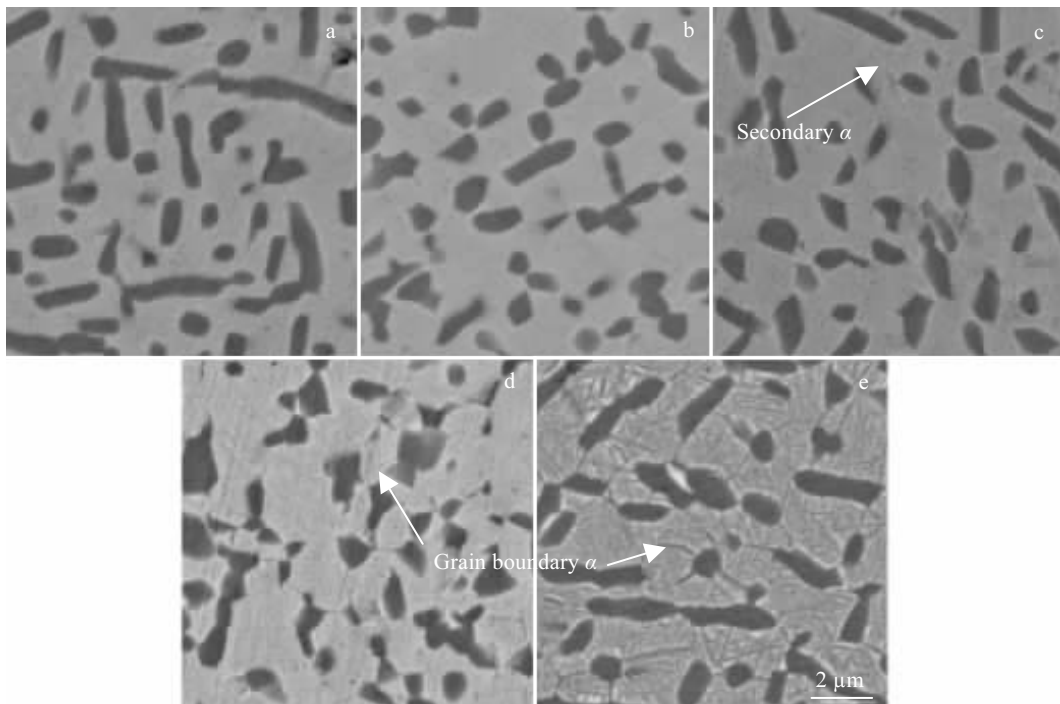
Fig.4   SEM images of the alloy after solution treatment at 850 °C and aging for 6 h at different temperatures: (a) 460 °C, (b) 500 °C, (c) 540 °C, (d) 580 °C, and (e) 620 °C
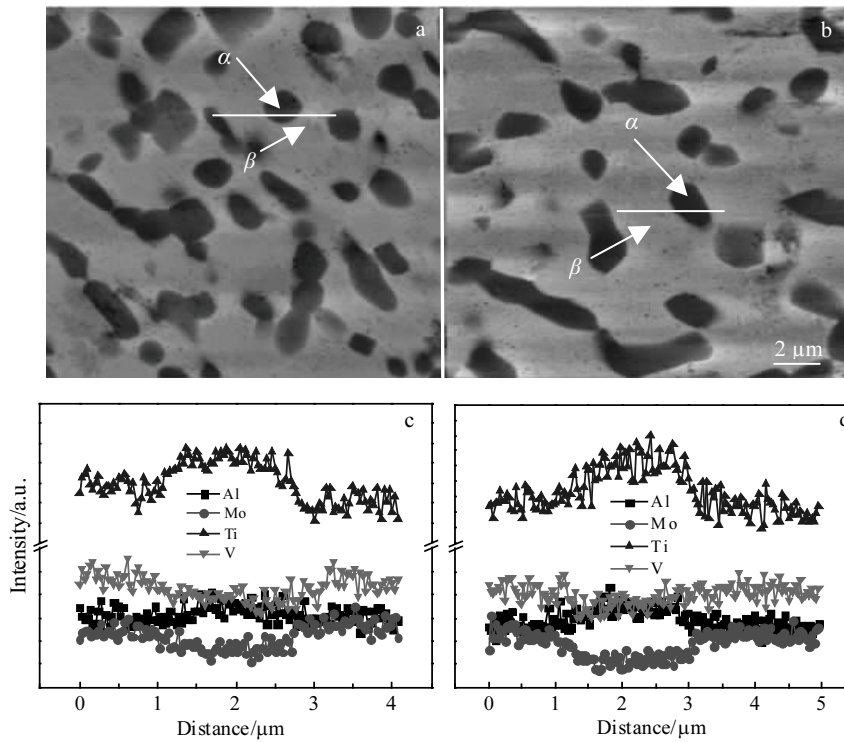
Fig.5　Microstructures (a, b) and EPMA line scanning (c, d) of the alloy solution treatment at 825 $^{\circ}$C (a) and 850 $^{\circ}$C (b) for 0.5 h: (c) the composition profiles along the line shown in Fig.5a; (d) the composition profiles along the line shown in Fig.5b
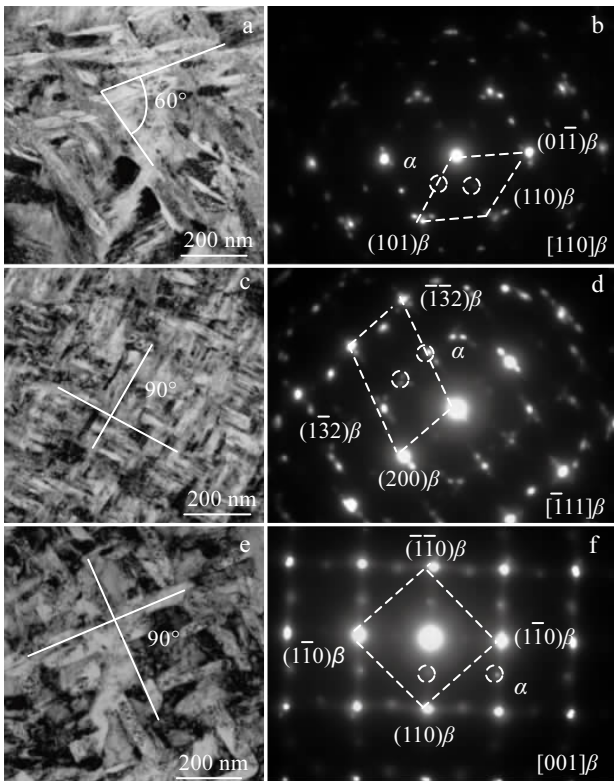
Fig.6　Bright-field images of the alloy solution treatment at 900 $^{\circ}$C and aged at different temperatures for 6 h: (a) 540 $^{\circ}$C; (c) 580 $^{\circ}$C; (e) 620 $^{\circ}$C; (b, d, f) are the selected area electron diffraction patterns for (a, c, e), respectively
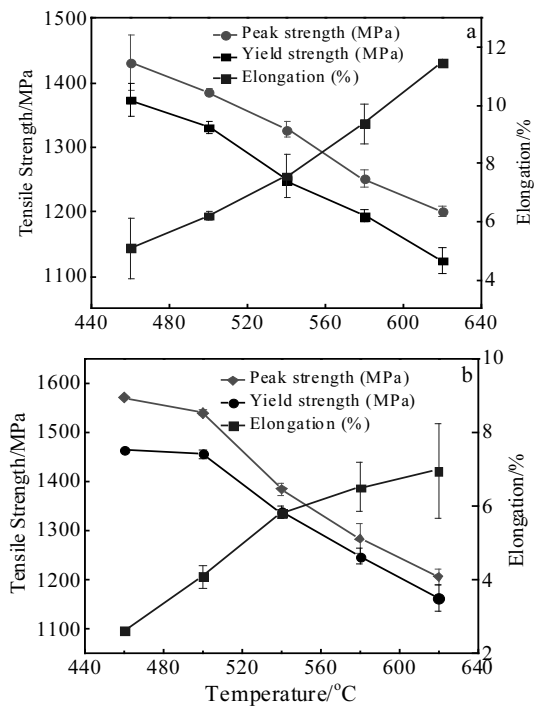
Fig.7　Tensile properties of the Ti-6Al-6Mo-4V alloy after solution treatment at various temperatures and aging at different temperatures for 6 h: (a) 825 $^{\circ}$C and (b) 850 $^{\circ}$C

Normally, the strength decreases and elongation increases with the increase in aging temperatures for solution treatment in α/β region plus aging conditions (Fig.7). The secondary α with a very small size in case of lower aging temperatures, which lead to the concentration of stress and cracks from grain boundary going through grains directly, thus resulting in high strength but poor elongation. After aging at higher aging temperatures, the strength reduces sharply because α phase precipitates and coarsens between β grains, and then cracks will propagate along α phase.

Table 2 illustrates the tensile properties of the alloy after solution treatment in β region plus aging. The strength rises to the peak and decreases with increase of aging temperatures, which is different from the trend after α/β region solution treatment in Fig.7. This phenomenon should be attributed to the difference of microstructures after aging at different temperatures. For example, in case of aging at 540 and 580 °C, a high strength level (1300~1410 MPa) is obtained but most of them with a poor elongation (~1.3%) because most of grains break during the stage of elastic deformation due to the existence of very fine and long α precipitating along with coarser β grains, which results in the occurrence of intergranular fracture. Further analysis will be presented in the next section. After aging at 620 °C, continuing coarsening of secondary α phase results in a lower strength (1292 MPa) and higher elongation (~2.0%).

Fig.8 presents the distribution map of strength and elongation for all kinds of heat treatments adopted. It is

clear to see that the alloy shows a higher strength and elongation after α/β region heat treatment (the circle spots). The reason is that the primary α after α/β solution treatment limits the β grains effectively. A small size grain is beneficial to the high strength according to the Hall-petch relationship. Furthermore, the elongation mainly depends on the resistance of crack nucleation, which is determined by the effective slip length parallel to the grain boundary α-layers, and a small size grain can effectively reduce the slip length and increase crack nucleation resistance.

2.3 Fractography

In order to identify fracture mechanism, several samples are selected for fractography studying.

Fig.9a and 9b show the fractographs of $\alpha+\beta$ region solution treatment plus aging and tensile testing samples. Aging at lower temperatures (460 °C) leads to a type of ductile fracture (Fig.9a) with shallow and deep dimples. Aging at 620 °C, a completely ductile fracture as shown in Fig.9b is obtained with fine and deep dimples with almost no facets. The trend is the same as solution treatment at 850 °C. Fig.10 and Fig.11 show the fractographs of β region solution treatment plus aging and tensile testing samples. Low aging temperature (540 °C) results in a mixed mode but mainly faceted intergranular type of fracture with small part of ductile fracture (Fig.10). And the concentration of high stress and high local strains at

Table 2 Tensile properties of the Ti-6Al-6Mo-4V alloy after solution treatment at 900 °C and aging for 6 h

Aging temperature/°C	R_m/MPa	$R_{p0.2}$/MPa	A/%
540	1300	1287	1.31
580	1410	1399	1.45
620	1292	1287	2.01
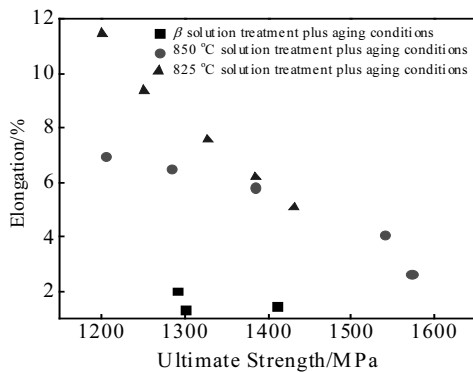
Fig.8   Plot of elongation and ultimate strength of Ti-664 in all solution treatment plus aging conditions
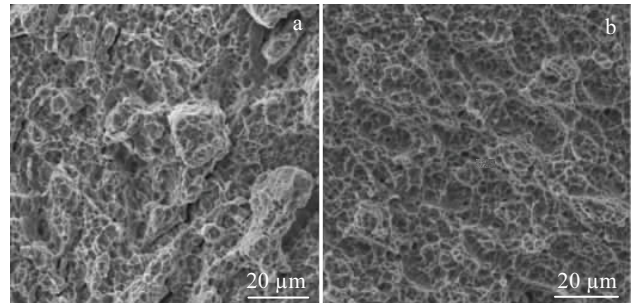
Fig.9   Fracture surface of the alloy after solution treatment at 825 °C plus aging at different temperatures for 6 h: (a) 460 °C and (b) 620 °C
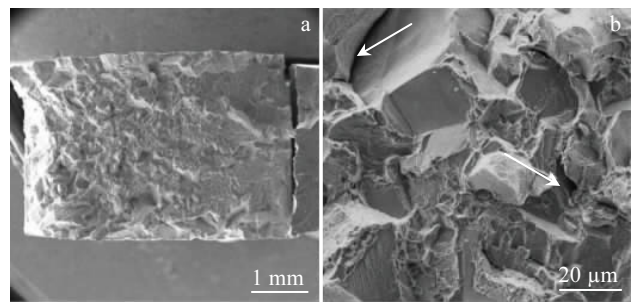
Fig.10   Fracture surface of the alloy after β solution treatment plus aging at 540 °C for 6 h: (a) overall fracture area and (b) magnified image
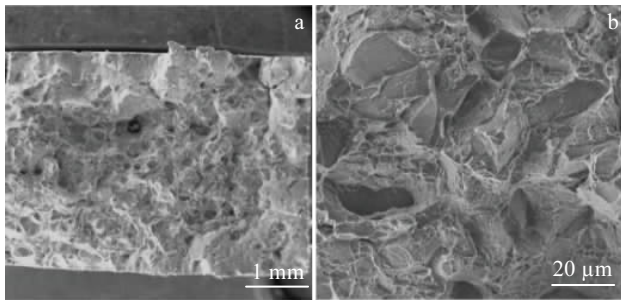
Fig.11 Fracture surface of the alloy after β solution treatment plus aging at 620 °C for 6 h: (a) overall fracture area and (b) magnified image

boundary triangle area results in separation of grains, as shown in Fig.10b. Furthermore, the smaller angle grain at triangle area is easy to bear a larger load than that of other two grains, so the separation is more likely to develop at the smaller angle grain (shown by arrows). After aging at 620 °C, the fracture shows mixed mode type but there are more dimpled regions surrounding the facets and almost no cracks (Fig.11).

3 Conclusions

1) The primary α of Ti6Al4V alloy forms after heat treatment when temperatures are below β transus, and the volume fraction primary α decreases and the size increases with the increase of solution temperatures. Solution treatment in β region leads to coarsening grains.

2) During aging treatment, the size of secondary α increases with the increase of aging temperatures. After aging at 460 °C, both α/β solution treatment plus aging conditions obtain the highest tensile strength. After aging at 540 °C, the alloy achieves the greatest combination of strength (1328 MPa) and elongation (7.58%) after solution treatment at 825 °C.

3) Fractography indicates that the β solution treatment plus aging specimens exhibits a mixed mode type of fracture surface, where specimens after α/β solution treatment plus aging show a dimpled fracture surface.

References

[1] Nag S, Banerjee R, Stechschulte J *et al*. *Journal of Materials Science Materials in Medicine*[J], 2005, 16 (7): 679

[2] Yan M Q, Sha A X, Li K *et al*. *Rare Metal Materials & Engineering*[J], 2017, 46(S1): 156

[3] Gouda M K, Nakamura K, Mohamed A H G. *Journal of Applied Physics*[J], 2015, 117(21): 214 905

[4] Du Z, Xiao S, Xu L *et al*. *Materials & Design*[J], 2014, 55(55): 183

[5] Reham R, Adel N, Abdel-Hamid H. *Metallography Microstructure & Analysis*[J], 2013, 2(6): 388

[6] Li C, Chen J, Li W *et al*. *Journal of Alloys & Compounds*[J], 2016, 684: 466

[7] Gao L , Liu J, Cheng X *et al*. *Materials Science & Engineering A*[J], 2014, 618: 104

[8] Huang X, Cuddy J, Goel N *et al*. *Journal of Materials Engineering & Performance*[J], 1994, 3(4): 560

[9] Zhou W, Ge P, Zhao Y *et al*. *Rare Metal Materials & Engineering*[J], 2017, 46(8): 2076

[10] Boyne A, Wang D, Shi R P *et al*. *Acta Materialia*[J], 2014, 64: 188

[11] Feng Y Z, Hong C, Yi K X *et al*. *Rare Metal Materials and Engineering*[J], 2013, 42(7): 1332

[12] Glatz S A, Koller C M, Bolvardi H *et al*. *Surface & Coatings Technology*[J], 2017, 311: 330

[13] Oliveira N T, Guastaldi A C. *Acta Biomaterialia*[J], 2009, 5 (1): 399

[14] Rodrigues A V, Oliveira N T, dos Santos M L *et al*. *Journal of Materials Science Materials in Medicine*[J], 2015, 26(1): 5323

[15] Jones N G, Dashwood R J, Jackson M *et al*. *Scripta Materialia*[J], 2009, 60(7): 571

[16] Dehghan-Manshadi A, Dippenaar R J. *Materials Science & Engineering A*[J], 2012, 552: 451

[17] Fan J K, Kou H C, Lai M J *et al*. *Materials & Design*[J], 2013, 49: 945

[18] Jackson M, Dashwood R, Flower H *et al*. *Metallurgical & Materials Transactions A*[J], 2005, 36 (5): 1317

[19] Saito T, Furuta T, Hwang J H *et al*. *Science*[J], 2003, 300 (5618): 464

[20] Sauer C, Lütjering G. *Materials Science & Engineering A*[J], 2001, 319 (1): 393

[21] SemiatinS L, Fagin P N, Glavicic M G *et al*. *Materials Science & Engineering A*[J], 2001, 299 (1): 225

热处理对新型高强钛合金组织与性能的影响

盛金文 [1]，王振宇 [1]，吴　迪 [1]，白卫民 [1]，章立钢 [1,2]，刘立斌 [1,3]

(1. 中南大学，湖南 长沙 410083)

(2. 德国弗莱贝格工业大学，德国 弗莱贝格 D-09596)

(3. 有色金属材料科学与工程教育部重点实验室，湖南 长沙 410083)

摘　要：研究了新型高强钛合金（Ti-6Al-6Mo-4V）的微观结构和力学性能。分别在 α/β 和 β 区固溶处理后，在 460~620 ℃ 5 个不同温度下时效 6 h，研究合金的组织与性能之间的关系。结果表明，α/β 区固溶时效处理后的性能与 β 单相区固溶时效处理后相比，α/β 区固溶时效处理后合金获得更好的强度和塑性组合。在 850 ℃（α/β 区域）固溶处理以及 460 ℃时效后，合金获得最高的强度为 1572 MPa，伸长率为 2.63%；在 620 ℃时效时，合金的伸长率达到最高为 11.46%，但强度较低为 1201 MPa。经过 825 ℃固溶处理，540 ℃时效后，该合金获得最好的强度（1328 MPa）和伸长率（7.58%）匹配。同时，β 区溶液处理后的 β 晶粒较大，时效后形成细小的二次 α 相，导致强度和塑性较差。

关键词：Ti-6Al-6Mo-4V；显微组织；力学性能；断口